In situ and laboratory results of a bentonite-based block/pellet seal during saturation

Arisleidy Mesa-Alcantara[1#] and *Enrique* Romero[1,2]

[1] *Geomechanics Group, International Centre for Numerical Methods in Engineering*
Gran Capità s/n, 08034 Barcelona, Spain.
[2] *Department of Civil and Environmental Engineering, Universitat Politècnica de Catalunya*
Jordi Girona 1-3, 08034 Barcelona, Spain.
[#]*arisleidy.mesa@upc.edu*

ABSTRACT

The in situ Engineered Barrier (EB) experiment aimed at understanding the hydromechanical behaviour of sealing materials for high-level radioactive wastes as a combination of compacted blocks and high-density pellets made of Febex bentonite. The experimental program focused on the wetting process of a heterogeneous dual-component sample consisting of pellets and blocks with technological gaps. The homogenisation tendency was investigated by determining the final (local) dry densities and pore size distributions in both zones from post-mortem analyses. Global initial dry densities between 1.36–1.44 Mg/m^3 were considered for the heterogeneous mixture, wetted at constant volume and constant vertical stress (oedometer conditions). The initially high-density zone of blocks with technological gaps expanded during hydration, reaching a lower dry density at saturation than the pellets' zone. The initially low-density pellets' zone with a high volume of inter-pellet pores underwent compression and reached a final high dry density on saturation. The experimental results were compared with the distribution of dry density at the in situ EB experiment after dismantling, and a good agreement between the laboratory and the in situ measurements was observed.

Keywords: Febex bentonite; in situ experiment; laboratory tests; block/pellet seal

1. Introduction

Bentonite-based heterogeneous mixtures of high-density crushed pellets and compacted blocks have been studied as suitable sealing materials for radioactive waste geological repositories because of their high swelling capacity and low water permeability. Compacted bentonite blocks have been used in demonstration projects, but emplacement operations are challenging to automate, and open voids are almost unavoidable. For this reason, pellet mixtures installed in horizontal drifts aim to improve emplacement operation and reduce the gaps around nuclear waste disposal canisters and host rock. In this context, an in situ Engineered Barrier (EB) experiment (Alonso and Hoffmann 2007, García-Siñeriz, Rey and Mayor 2008, Palacios et al. 2013) launched in the underground laboratory of Mont Terri (Switzerland) aimed at demonstrating a new concept for the construction of bentonite-based seals in competent clay formation (Opalinus clay). This concept was based on using a lower bed of heavily compacted Febex bentonite blocks ($\rho_d \approx 1.70$ Mg/m^3), and an upper zone of crushed pellets emplaced using an auger ($\rho_d = 1.36$ Mg/m^3). A schematic of the EB experiment is shown in Figure 1, with a steel dummy canister placed in the centre surrounded by an artificial hydration system to reduce saturation time.

The experiment was dismantled in 2014 after almost 12 years of hydration (Palacios et al. 2013). Laboratory tests were performed on samples taken from several cross-sections to check the dry density of the components after long-term hydration. The block zone reduced the dry density, and the pellet mixture showed the opposite behaviour with increased dry density.

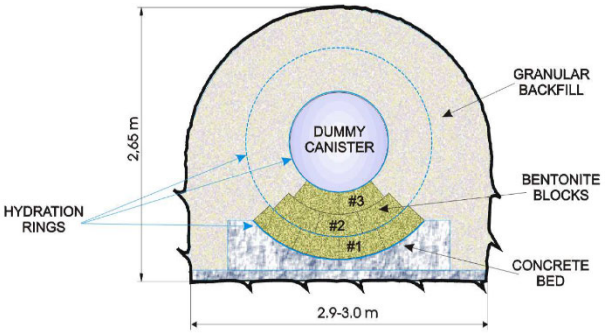

Figure 1. Cross-section of in situ EB experiment with heterogeneous seal and hydration rings (Palacios et al. 2013).

The current study mimicked this in situ experiment by investigating the homogenisation trend during wetting heterogeneous dual-component samples of Febex pellets and blocks with technological gaps. The pellets were installed at a dry density of 1.30 Mg/m^3, whereas the block zone with gaps reached dry densities between 1.42 and 1.58 Mg/m^3. The investigation focused on performing tests under constant volume and constant vertical stress under oedometer conditions (Mesa-Alcantara 2014). The homogenisation trend was investigated by determining the two zones' final (local) dry density, complemented by mercury intrusion porosimetry tests to define the final pore size distributions. The results confirmed a final state towards

partial homogenisation with a lower gradient of dry density between the two distinct zones, consistent with the in situ observations.

2. Tested material

2.1. Febex bentonite

Febex bentonite has a solid density of 2.70 Mg/m^3, a liquid limit of 102%, a plastic limit of 53%, and 67% of particles are smaller than 2 µm (Villar and Lloret 2007; Hoffmann, Alonso, and Romero 2007). The cation exchange capacity is 102 meq/100g, with calcium (35 meq/100g), magnesium (31 meq/100g), and sodium (27 meq/100g) as the main exchangeable cations.

Bentonite pellets were fabricated from Febex bentonite. The powder was preheated at 120ºC and then heavily compacted. As a result, high dry-density granules (dry density of 1.90 Mg/m^3) were obtained at low water content (3-4%), corresponding to a total suction between 250–300 MPa. Finally, the granules were broken and sorted by size. They were mixed according to a modified Fuller curve described below.

2.2. Sample preparation

The heterogeneous dual-component sample was formed by pellets (1.30 Mg/m^3) and heavily compacted blocks with a dry density of 1.65 Mg/m^3. The sample size for all tests was 50 mm in diameter and 20 mm in height. The pellet mixture was statically compacted directly in an oedometer ring, and the blocks were placed after leaving the technological gaps.

The pellets' grain size distribution was adjusted to D_{max} = 4.76 mm. Fuller's particle size distribution was used to avoid segregation during pouring because it optimises packing and dry density. The curve plotted in Figure 2 was determined using the following expression

$$P = \frac{\sqrt{D/D_{max}} - \sqrt{D_{min}/D_{max}}}{1 - \sqrt{D_{min}/D_{max}}} \quad (1)$$

where P represents the mass fraction passing, D is the pellet size, and D_{min} = 0.42 mm is the corresponding minimum pellet size.

The pellet's dry density was 1.90 Mg/m^3, its water content ranged between 8.4 and 10.2%, and its degree of saturation extended between 53.9 and 65.4%.

The pellet mixture was statically one-dimensionally compacted at a constant vertical displacement rate of 0.1 mm/min at slightly higher water of 5.3% until reaching a dry density of 1.30 Mg/m^3 (void ratio of 1.08, porosity of 0.52), which required a vertical stress around 2 MPa. The pellet zone's initial (local) degree of saturation is 13.3%.

The powder passing through the ASTM#40 sieve (0.425 mm) at a water content of 12% was used to prepare the blocks at a dry density of 1.65 Mg/m^3 using a similar static compaction process. Typical fabrication (vertical) stresses were between 40 and 50 MPa for blocks at dry densities between 1.69 and 1.70 Mg/m^3 and at a total suction between 100 and 150 MPa (Lloret and Villar 2007). The block zone of 10 mm in height consisted of nine blocks with a maximum spacing of 1 mm between them (technological gaps). The dry density of this zone varied between 1.42 and 1.58 Mg/m^3. This separation between blocks also allowed for fast hydration. The two components of the sample were separated with a metallic mesh for a more accessible partition after the hydration. Figure 3 shows the heterogeneous dual-component configuration.

Two different configurations of the sample were used to perform the tests. The difference stemmed from considering the material in contact with the bottom hydration boundary. In the first configuration (FC), the blocks were placed at the bottom, mimicking the organisation of the in situ experiment. In the second configuration (SC), the pellets were in contact with the bottom hydration boundary.

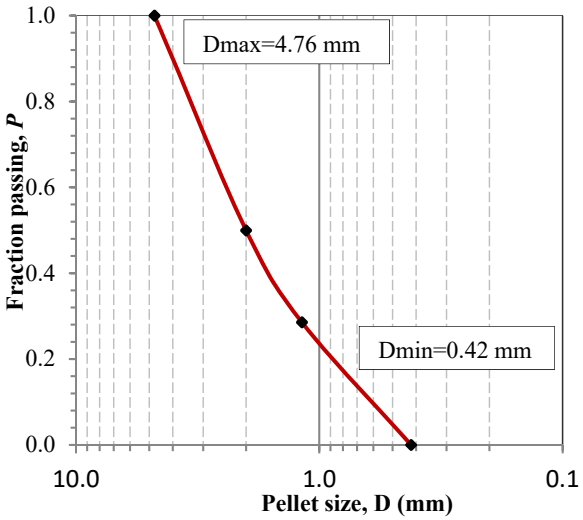

Figure 2. Particle size distribution of the pellets.

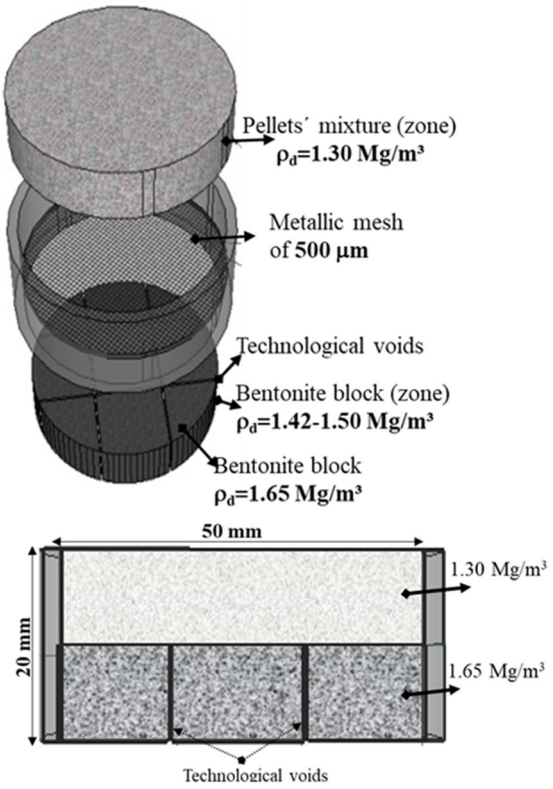

Figure 3. Heterogeneous dual-component configuration of the tests (FC).

3. Experimental setup and protocols

3.1. Constant volume wetting (CVW) tests

Eight tests were performed at constant volume using the isochoric cell shown in Figure 4. An automatic pressure/volume controller was used to inject and pressurise water at the bottom of the sample. The water pressure applied in the different tests ranged between 100 kPa and 2 MPa. Both configurations (FC and SC) were used in these tests. The hydration lasted more than 15 days to ensure complete saturation.

The difference in the block's dry density zone is due to the technological voids, which varied between 1.02 and 2.97 cm^3. Table 1 summarises the samples' initial conditions before saturation. The overall degree of saturation was estimated as

$$S_r = \frac{S_{rp} n_p + S_{rb} n_b}{n_p + n_b} \quad (2)$$

where S_{rp} = 0.133 and n_p = 0.52 are the pellet's zone degree of saturation and porosity, and S_{rb} and n_b are the corresponding values of the block's zone.

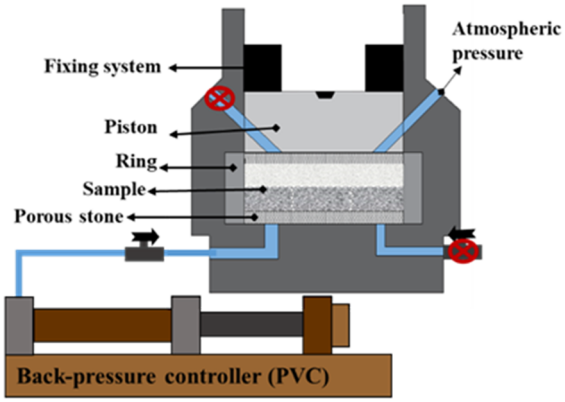

Figure 4. Constant volume cell and pressure/volume controller.

Table 1. Initial conditions of the CVW tests.

Sample	Dry density (Mg/m^3) Void ratio (e)		Degree of saturation (%)	
	Block zone	Overall sample	Block zone	Overall sample
Test 1 (FC)	1.56 0.73	1.43 0.89	44.4	27.2
Test 2 (FC)	1.58 0.71	1.44 0.88	45.6	27.7
Test 3 (SC)	1.48 0.82	1.39 0.94	39.5	25.4
Test 4 (SC)	1.45 0.86	1.38 0.96	37.7	24.7
Test 5 (FC)	1.46 0.85	1.38 0.96	38.1	24.9
Test 6 (SC)	1.42 0.90	1.36 0.99	36.0	24.1
Test 7 (FC)	1.42 0.90	1.36 0.99	36.0	24.1
Test 8 (FC)	1.50 0.80	1.40 0.93	40.5	25.8

3.2. Constant vertical stress wetting (CVSW) tests

Three oedometer tests at constant vertical stress and under FC were carried out at 1, 2, and 3 MPa. Water was pressurised at the bottom boundary of the cell using a PVC controller at a water back-pressure of 50 kPa to 2 MPa. The hydration lasted less than 20 days. Table 2 shows the samples' initial condition. Figure 5 presents the oedometer testing device.

Table 2. Initial conditions of constant vertical stress tests.

Test vertical stress	Dry density (Mg/m^3) Void ratio (e)		Degree of saturation (%)	
	Block zone	Overall sample	Block zone	Overall sample
Test 1 1 MPa	1.41 0.91	1.36 0.99	35.6	24.0
Test 2 2 MPa	1.43 0.89	1.37 0.97	36.4	24.3
Test 3 3MPa	1.46 0.85	1.38 0.96	38.1	24.9

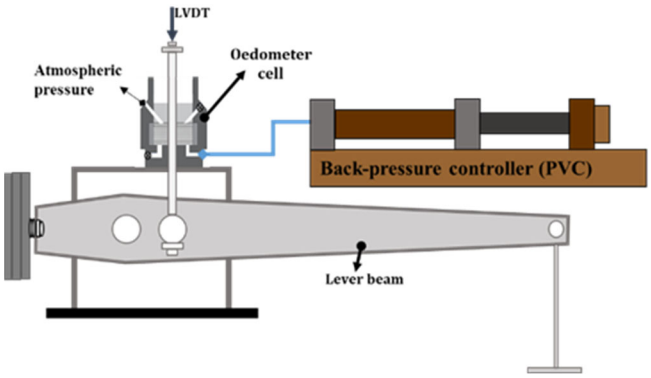

Figure 5. Oedometer cell and pressure/volume controller.

3.3. Determination of bulk density and pore size distributions of the components after saturation

The paraffin wax method was used to determine the components' final (local) bulk densities after saturation. The water content was determined after 2-day oven drying on parallel samples, which allowed for determining the dry densities of the components.

The pore size distribution with mercury intrusion porosimetry MIP (Micrometrics Auto Pore IV 9500) was performed on freeze-dried samples retrieved after long-term hydration. Washburn equation (Eq. 3) was used to provide a relationship between the applied (absolute) non-wetting mercury pressure (p_{nw}) and the entrance pore size x (σ_{nw} = 0.484 N/m at 25ºC is the surface tension of non-wetting mercury, and θ_{nw} = 140º the contact angle between mercury and particle surface) (Romero and Simms 2008). The pore size density (PSD) function was determined using Eq. 4. (e_{int} represents the intruded void ratio, volume of intruded mercury to the volume of solids)

$$p_{nw} = -\frac{4\sigma_{nw} \cos\theta_{nw}}{x} \quad (3)$$

$$PSD = -\frac{de_{int}}{d\log x} \quad (4)$$

4. Experimental results

4.1. Constant volume wetting tests

After long-term saturation, each test was carefully dismantled. The final (overall) dry density reached the same value as the initial (overall) dry density in all tests. Different behavioural features were detected in the various components. After hydration, the high-density block zone with technological gaps swelled and decreased the final (overall) dry density between 1.29 and 1.40 Mg/m^3, as shown in Figure 6. However, the opposite behaviour was observed in the pellets' zone, which was compressed by the block zone, inducing an increase in the final dry density (1.38 and 1.46 Mg/m^3). The evolution of the dry density of the pellets' zone is summarised in Figure 7. It is important to remark that high and low dry densities were exchanged during the wetting process: the final (local) dry density of the pellets' zone ended with a higher value despite starting from a lower density value.

The results confirmed a final state towards partial homogenisation with a lower dry density gradient between the two distinct zones. The initial difference between the low and high-density zones ranged between 0.11 to 0.28 Mg/m^3, whereas at saturation, this difference reduced to 0.06 to 0.17 Mg/m^3.

Despite the lower scale of the experimental results, the data were consistent with the EB experiment after dismantling.

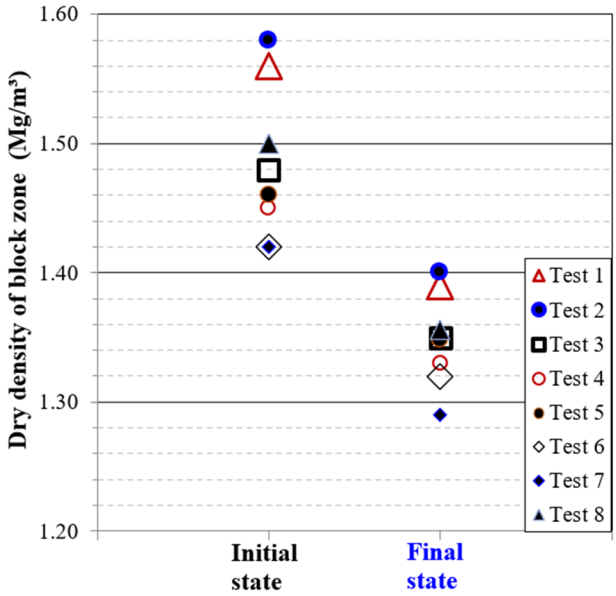

Figure 6. Dry densities of block zone at initial and final states (constant volume tests).

The values of the block and pellets' final dry density were used to estimate the swelling pressure using the data reported by Hoffmann, Alonso and Romero (2007) and Lloret and Villar (2007). Figure 8Fndra indicates that the pellets' zone tried to reach a welling pressure between 1 and 2 MPa. Nevertheless, the block zone tended to lower estimated swelling pressures between 0.7 and 1.5 MPa. This is not entirely consistent. Nonetheless, it allowed estimating a swelling pressure range of the swelling pressure of the dual-component mixture between 1 and 2 MPa. These values will be discussed later based on the volume change behaviour of the dual-component mixture on wetting at different vertical stresses.

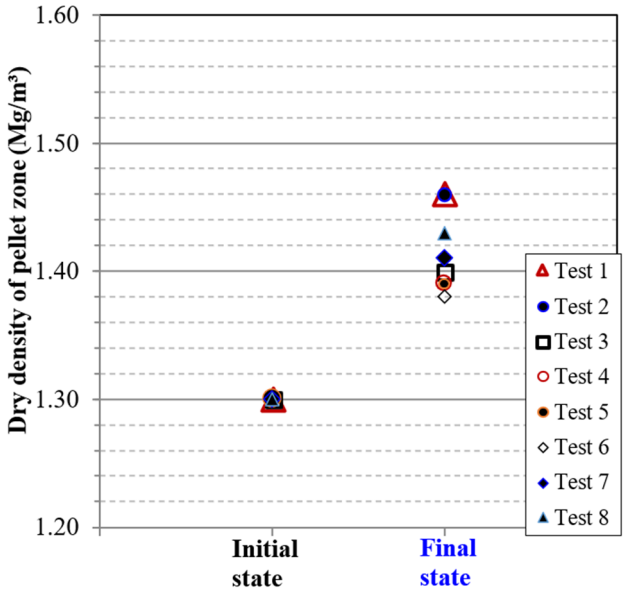

Figure 7. Dry densities of pellets' zone at initial and final states (constant volume tests).

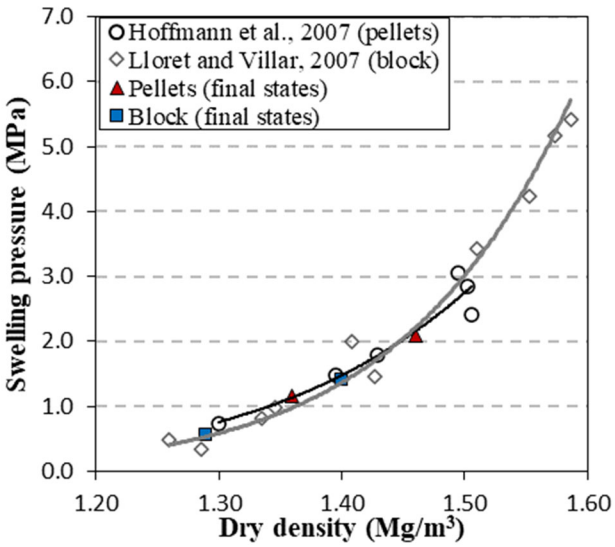

Figure 8. Estimated swelling pressure of the components based on data reported by different authors (Hoffmann 2007; Lloret and Villar 2007).

4.2. Constant vertical stress wetting tests

Figure 9 presents the axial strain evolution on loading and wetting at constant vertical stresses. Only the test at 1 MPa displayed a swelling of -1.70% (swelling strains are negative). Collapse deformations were observed at 2 and 3 MPa, with 2.3% and 3.6% axial strains, respectively. These results allowed estimating a swelling pressure of around 1.3 MPa for the dual-component

mixture during wetting, consistent with the values reported in Figure 8 for the two components.

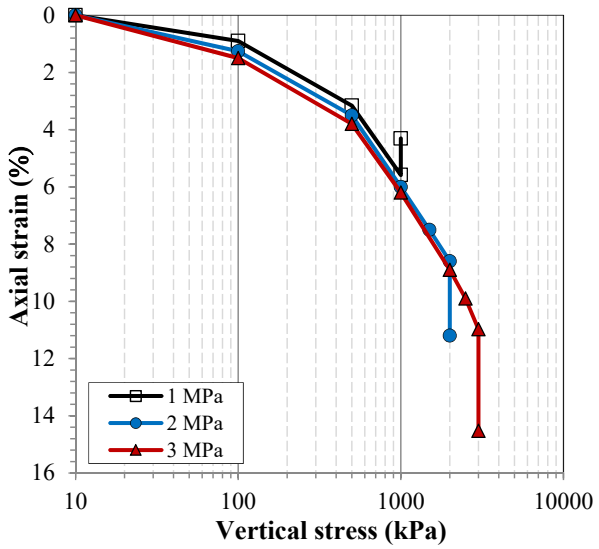

Figure 9. CVSW tests. Axial strain versus vertical stress on loading and wetting.

4.3. Microstructural behaviour after wetting paths

The dual-component mixture displayed a multi-modal pore size distribution PSD function that significantly evolved during saturation. The pellets' zone initially displayed large inter-pellet voids (around 250 µm), as well as inter-aggregate and intra-aggregate pores between and inside aggregates of the order of 3 µm and 13 nm, respectively, for a mixture of pellets of 1.2 Mg/m^3 (Alonso, Romero and Hoffmann 2011). The block zone showed large technological gaps with a maximum size of 1 mm, and inter-aggregate and intra-aggregate pores inside the block. The dominant pore sizes corresponded to inter-aggregate pores of the order of 20 µm and intra-aggregate pores of 20 nm (Lloret and Villar 2007), which are slightly larger than the pellets (dry density 1.90 Mg/m^3) due to the lower dry density of the block.

Figure 10 shows the PSDs of the block and pellet zones after wetting at constant volume (CVW). As observed, the block zone underwent a significant swelling with a dominant pore size of 510 nm. In contrast, the pellet's zone underwent significant compression by mainly reducing the inter-pellet pores (a small peak was still observed at around 30 µm). The inter-aggregate and intra-aggregate pore sizes were similar to the ones reported by Alonso, Romero and Hoffmann (2011): 4.4 µm for the inter-aggregate and 13 nm for the intra-aggregate voids.

Nevertheless, in the CVSW-1MPa test shown in Figure 11, the pellets' zone displayed dominant pores between 0.7 and 0.8 µm, indicating that the material underwent a substantial swelling and a reduction in the macroporosity (some macroporosity was still present at sizes > 10 µm in both components). This fact was consistent with the local swelling of the pellets' zone determined from post-mortem dry density analyses, which suggested a significant swelling of around 10.1% (part of this swelling was also observed in Figure 9 in terms of the expansion undergone by the dual-component mixture at 1 MPa).

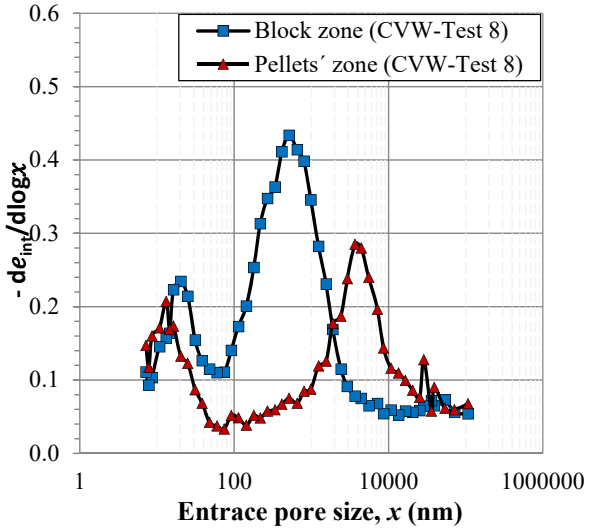

Figure 10. Pores size distribution of the components after saturation from constant volume tests.

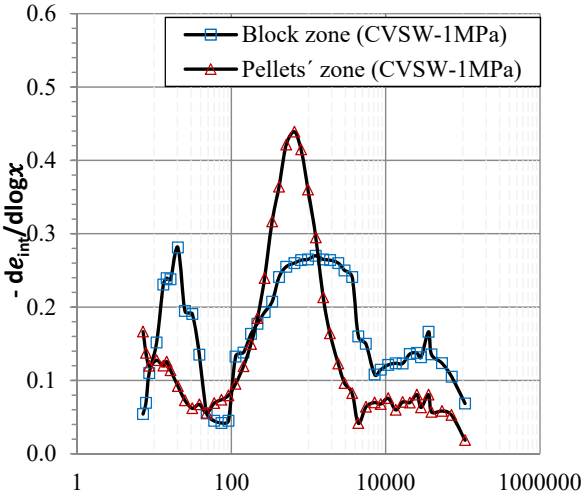

Figure 11. Pores size distribution of the components after saturation from constant vertical stress tests at 1 MPa.

5. Concluding remarks

The dual-component mixture consisting of pellets and blocks with technological gaps exhibited a complex response when wetted. An experimental program was launched to observe the homogenisation tendency by determining the final (local) dry densities and pore size distributions in both components under constant volume conditions from post-mortem analyses.

When measuring the components' initial and final dry densities, some tendency towards homogenisation was detected in these constant volume hydration tests. The initial difference between the low and high-density components ranged between 0.11 and 0.28 Mg/m^3, whereas at saturation under constant volume, this difference reduced to 0.06 to 0.17 Mg/m^3. The initially dense bentonite blocks with technological gaps (dry

densities between 1.42 and 1.58 Mg/m^3) evolved during saturation at constant volume towards a looser material due to swelling. In contrast, the pellets' zone experienced a significant dry density increase due to compression on wetting. The initially high-density zone of blocks reached a lower dry density at saturation than the pellets' zone.

The experimental results were compared with the distribution of dry density at the in situ EB experiment after dismantling (Palacios et al. 2013), and a good agreement between the laboratory and the in situ measurements was observed despite the different scales involved, as presented in Figure 12.

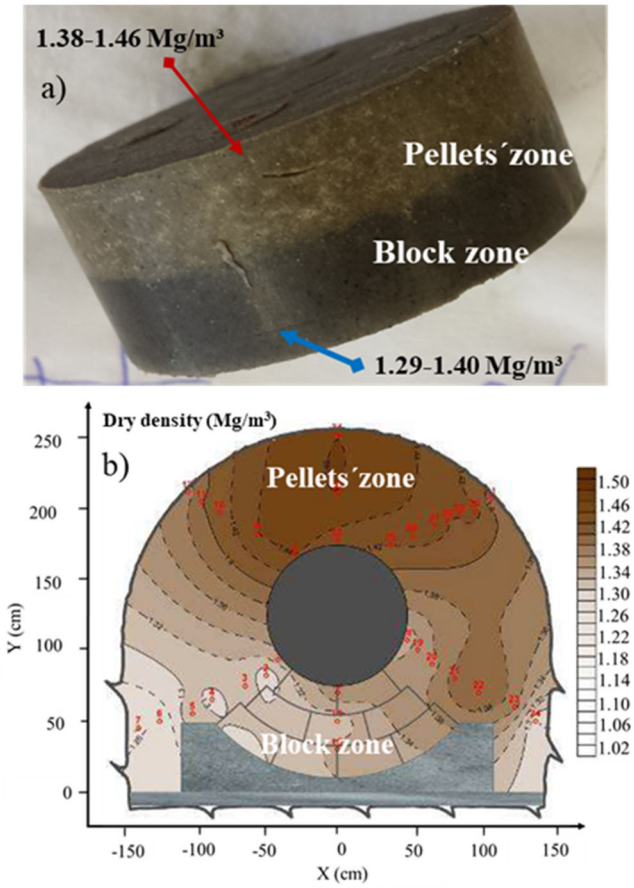

Figure 12. Final local dry density comparison between EB experiment results after dismantling and experimental results of this study.

Acknowledgements

The authors wish to acknowledge the support provided by ENRESA, the Spanish National Agency for Nuclear Waste Disposal.

References

Alonso, E.E. and C. Hoffmann. 2007. "Modelling the Field Behaviour of a Granular Expansive Barrier." Physics and Chemistry of the Earth, Parts A/B/C 32 (8–14): 850–65. https://doi.org/10.1016/j.pce.2006.04.039.

Alonso, E., E. Romero, and C. Hoffmann. 2011. "Hydromechanical Behaviour of Compacted Granular Expansive Mixtures: Experimental and Constitutive Study." Géotechnique 61 (4): 329–44. https://doi.org/10.1680/geot.2011.61.4.329.

Hoffmann, C., E. Alonso, and E. Romero. 2007. "Hydro-Mechanical Behaviour of Bentonite Pellet Mixtures." Physics and Chemistry of the Earth, Parts A/B/C 32 (8–14): 832–49. https://doi.org/10.1016/j.pce.2006.04.037.

García-Siñeriz, J.L., M. Rey, and J.C. Mayor. 2008. "The engineered barrier experiment at Mont Terri Rock Laboratory,". *Science and Technology Series*, (334), 65-75

Lloret, A., and Villar, M.V. 2007. "Advances on the Knowledge of the Thermo-Hydro-Mechanical Behaviour of Heavily Compacted 'FEBEX' Bentonite." Physics and Chemistry of the Earth 32 (8–14): 701–15. https://doi.org/10.1016/j.pce.2006.03.002.

Mesa-Alcantara, A. "Mezclas de bloques y pellets de bentonita Febex. Estudio de densidades secas después de una etapa de humedecimiento," Master thesis in spanish Universitat Politècnica de Catalunya. http://hdl.handle.net/2099.1/24218.

Palacios, B., M. Rey., J.L. García-Siñeriz., M.V. Villar J.C. Mayor, and M. Velasco. 2013. Long-term Performance of Engineered Barrier Systems PEBS Engineered Barrier Emplacement Experiment in Opalinus Clay: 'EB' Experiment. As-built of dismantling operation," pp. 1–99, 2013.

Romero, E., and P. Simms. 2008. "Microstructure Investigation in Unsaturated Soils: A Review with Special Attention to Contribution of Mercury Intrusion Porosimetry and Environmental Scanning Electron Microscopy." Geotechnical and Geological Engineering 26 (6): 705–27. https://doi.org/10.1007/s10706-008-9204-5.

Villar, M.V., and A, Lloret. 2007. "Dismantling of the First Section of the FEBEX in Situ Test : THM Laboratory Tests on the Bentonite Blocks Retrieved." Physics and Chemistry of the Earth, Parts A/B/C 32 (8–14): 716–29. https://doi.org/10.1016/j.pce.2006.03.009.